Low-temperature thermal conductivity of bcc ^{3}He

A. S. Greenberg* and G. Armstrong†
Department of Physics, Colorado State University, Fort Collins, Colorado 80523
(Received 30 January 1979)

The thermal conductivity of bcc ^{3}He has been measured between 30 and 600 mK for a wide range of molar volumes. For carefully grown samples, the conductivity exhibited a T^3 temperature dependence. This dependence is characteristic of diffuse phonon boundary scattering with a temperature-independent mean free path, and a phonon specific heat which is in agreement with calorimetry measurements on bulk bcc ^{3}He. We were also able to grow samples for which the temperature dependence of the conductivity was less than cubic. These results are interpreted as the presence of another phonon-scattering mechanism in addition to boundary scattering. This scattering mechanism has a temperature dependence suggestive of edge dislocations in crystals. Several variations in sample growth techniques were performed, and these results support our interpretation of the presence of structural crystalline defects.

I. INTRODUCTION

The dependence of the thermal conductivity on temperature for a crystalline dielectric material is sensitive to the various phonon transport and scattering mechanisms, and is hence an excellent diagnostic for the concentration and nature of crystalline defects. In the limit of very low temperatures, the phonon velocity v becomes essentially constant, and the phonon wavelength λ, becomes sufficiently long that phonon scattering at a crystalline or a sample boundary dominates the heat-transport process. The thermal conductivity is then independent of the microscopic details of the crystal, and for a crystalline dielectric for which the phonons can be considered as a noninteracting gas, the thermal conductivity is proportional to the specific heat, C_v. In a Debye dielectric solid, $C_v \propto T^3$ for $T \ll \Theta$, where Θ is the Debye temperature. A straightforward relationship for the above-mentioned quantities is provided by the kinetic equation

$$k = \tfrac{1}{3} C_v v \lambda \ . \tag{1}$$

Theoretically, in a highly anharmonic crystal, such as bcc ^{3}He, phonons are not well-defined excitations, and Eq. (1) may not be rigorously valid. However, for experimental purposes, it greatly simplifies matters to consider phonons as the elementary thermal excitations, even in bcc ^{3}He. In fact, as we shall show, Eq. (1) is found to be consistent with our experimental results.

The only thermal-conductivity measurements taken close to the boundary scattering limit in bcc ^{3}He which have been previously reported are those of Thomlinson.[1] Although his samples had molar volumes that were 10% less than the largest possible, where anharmonic effects should be the greatest, he observed a thermal conductivity that decreased less quickly than T^3 in the boundary scattering limit; specifically, $k \sim T^{2.6}$. At that time, this result appeared to be in agreement with calorimetry data[2] which also reported an anomalously large specific heat in the bcc phase, and was tentatively thought to be related to the highly anharmonic nature of bcc ^{3}He. While there was perhaps qualitative agreement between the early heat-transport results and the calorimetry measurements, there did not exist any physical model which could quantitatively account for the noncubic behavior of both k and C_v at low temperatures.

Later specific-heat studies of Castles and Adams[3] quantified the anomalous contribution to the ^{3}He phonon specific heat as being linear in temperature. In 1976, however, Greywall[4] published very careful measurements of the bcc ^{3}He specific heat, and he found that $C_v \propto T^3$ in bulk samples of several molar volumes. He suggested that previous anomalous specific-heat results could be connected with size effects due to the presence of a large surface area in the calorimeters of the other researchers. This explanation would not be applicable to the thermal-conductivity measurements of Thomlinson, because he found the noncubic temperature dependence using a sample chamber geometry of comparable dimensions to that of Greywall's.

We would like to review for the reader that neither the specific-heat data of Castles and Adams, or the more recent data of Greywall, could be used to explain the thermal-conductivity results of Thomlinson. We illustrate the comparative status of these measurements in Fig. 1. In addition to Thomlinson's data

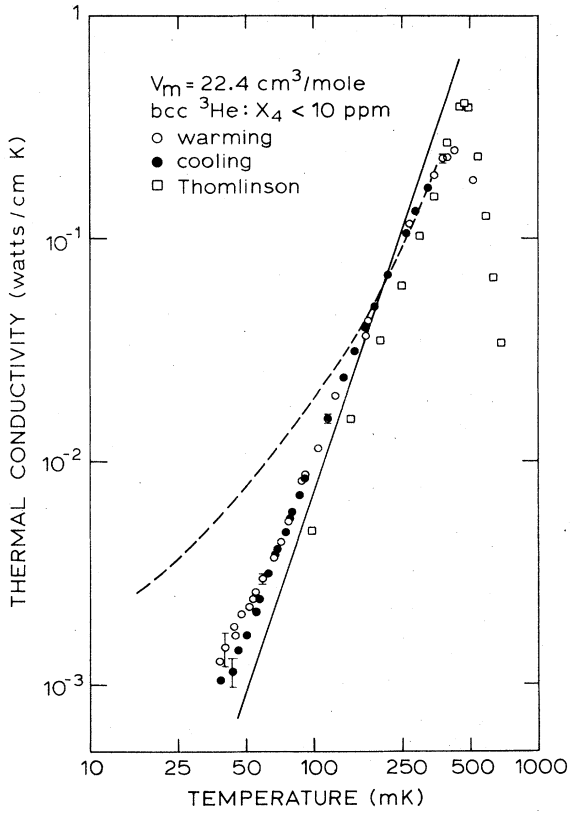

FIG. 1. Comparison of thermal-conductivity measurements at $v_m = 22.4$ cm^3/mole with a thermal conductivity generated using the specific heat of Castles and Adams (dashed line) and Greywall (solid line). The generated curves were adjusted by choosing the value of the mean free path at 200 mK to agree with our data and to give the best overall agreement with experiment.

at 22.4 cm^3/mole, we also show the results of our measurements at the same molar volume. After adjusting for differences in mean free path, our data reproduces the temperature dependence of the conductivity, $k \sim T^{2.6}$, found by Thomlinson. Our results further extend the conductivity measurements to nearly an order of magnitude lower temperature. We will explain other features of our data later in the text.

The dashed line in Fig. 1 was generated from Eq. (1) using the specific-heat data of Castles and Adams. We used the expression $C_v = \beta T + \alpha T^3$, where $\beta = 0.28$ mJ/cm^3 K^2 and $\alpha = 6.7$ mJ/cm^3 K^4. The latter value was taken from the specific-heat measurements of Greywall which is in agreement with the nonanomalous part measured by Castles and Adams. The conductivity generated using Greywall's specific-heat values is plotted as the solid line in Fig. 1. In both cases we have scaled the generated conductivities to agree with our measured conductivity at 200 mK.

As can be seen in this figure, there does not exist reasonable agreement between the two types of measurements in the low-temperature region. It is this discrepancy that motivated us to undertake careful thermal-conductivity measurements for molar volumes larger than previously have been measured, and to extend measurements to lower temperatures.

In our work, we have found the thermal conductivity varies as T^3 in many cases, and we conclude this Debye behavior is the fundamental temperature dependence. We believe that deviations from the cubic dependence observed by Thomlinson and ourselves are due to an additional phonon-scattering mechanism rather than anomalous specific-heat behavior.

II. EXPERIMENTAL ARRANGEMENT

Two different sample cells of basically similar design were used in this experiment. The first cell had a sample space diameter of $D_1 = 3.84$ mm and has already been described in detail elsewhere.[5] The second cell had a diameter $D_2 = 3.07$ mm, and is shown in Fig. 2. In this cell, we deleted the NMR

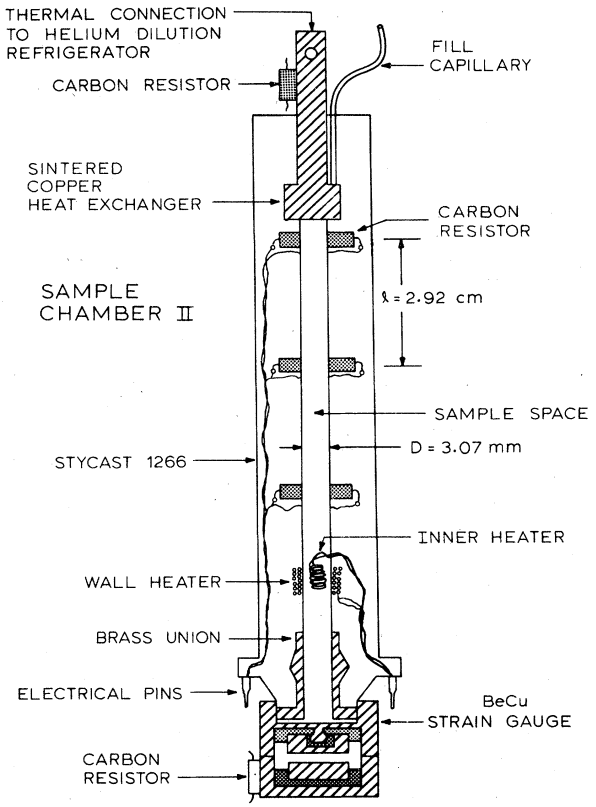

FIG. 2. Sample chamber was fabricated in a multistep process. The parts were joined using additional Stycast 1266 epoxy.

coils which were included in the first cell, and retained only a lower concentric heater imbedded in the wall. In the second cell we also included an additional heater suspended in the helium space. Furthermore, we redesigned the interface between the Stycast 1266 epoxy and the beryllium-copper strain gauge. The present design proved to be much more reliable at pressures higher than 100 atm.

In this article we only want to summarize relevant experimental aspects common to both sample chambers. The reader is referred to Ref. 5 for details of the sample chamber design and the calibration of the carbon thermometers.

The cylindrical sample cells were cast from Stycast 1266 epoxy with three 100 Ohm Speer resistors used for thermometry embedded in the epoxy. A circumferential cut was taken out of each resistor allowing the helium in the sample space to be in direct contact with the thermometer. These carbon resistors were calibrated by forming a liquid-solid mixture of ^{3}He and relating the equilibrium temperature to the melting pressure as recorded by the strain gauge. The equilibrium temperatures were then determined from composite melting curve data published in a review article by Trickey, Kirk, and Adams.[6]

There is nearly a 5% difference in the various determinations of the melting curve below the minimum temperature, $T_m = 0.318$ K. However, the accuracy of the thermometry is enhanced by fitting the resistor to a Mott hopping model using the functional form[7] $R = R_0 \exp(AT^{-1/4})$. The largest uncertainty in the thermal-conductivity data comes from taking the temperature difference between two thermometers ΔT, and the uncertainty varies inversely with ΔT. We have, therefore, the largest uncertainty around the conductivity peak and at very low temperatures where only a low heater power can be used to sustain the gradient. The conductivity data in Figs. 1 and 3 – 6 have error bars shown at representative points. Very low-temperature data points were cutoff when the uncertainty exceeded 30%.

The average thermal conductivity between any two thermometers was computed from

$$k = \frac{\dot{Q} l}{\Delta T A} \quad . \tag{2}$$

The quantity A/l is the ratio of the helium sample cross section to the distance between the thermometers. A four-wire method was used to measure $\dot{Q}$, the heater input power.

The average thermal conductivity defined by Eq. (2) will be different from a thermal conductivity associated with the average temperature, $k(T_{\rm av})$, where

$$T_{\rm av} = T_{\rm colder} + \Delta T/2 \quad .$$

If $k \sim T^3$, the fractional difference[8] varies as $\delta k/k \sim \frac{1}{4}(\Delta T/T_{\rm av})^2$, and in our experiments this is always less than 1%. A more important correction is the thermal conductance of the Stycast 1266. The empty sample chamber conductivities were measured for both sample cells, and the conductivity values of the helium which we report have been corrected for the epoxy conductivity.[5]

Our cells both had three thermometers which in principle allows us to compare two independent thermal paths; i.e., between the upper and middle resistor, and between the middle and lower resistor. However, the results for the lower path depended on which of the two heaters was used. We attribute this to a difference in the local temperature gradients and boundary resistances in the immediate vicinity of the heaters. For example, the heater embedded in the epoxy is surrounded by a material which has a conductivity that varies as T^2 while the solid helium conductivity varies as T^n, where n can be between 2.5 to 6 for temperatures below the conductivity peak. For most temperatures in this experiment, there are also several orders of magnitude difference between the values of the conductivity of the Stycast 1266 and the helium samples. However we expect that after a distance, on the order of several sample chamber diameters, the phonon flow will be independent of the local temperature gradients in the vicinity of the heater. We also observed that the upper and lower path difference depended on the particular helium sample in the chamber.

We mention this path-dependent conductivity because comparison of the two thermal-conductivity paths has been a common technique in determining the crystal quality. For example, Hogan *et al.*[9] used the criterion that a crystal was "unsplit" when the upper and lower paths differed by less than 10% and this criterion determined the selection of samples used in their data analysis. We would like to point out that the local environment and the proximity of the heater to the thermometers can have an important effect on the thermal-conductivity measurements. In this paper, we only report measurements for the upper thermal path which is independent of the particular heater used.

All the samples were grown using the blocked capillary technique. This allowed us to form molar volumes close to melting. The molar volumes were determined by measuring the pressure of the sample using the strain gauge and relating the pressure to molar volume from the melting curve data of Grilly.[10] As will be seen, using the blocked capillary technique we were able to grow crystals similar in quality to those grown using constant pressure techniques. The crystal quality was determined by the magnitude of the thermal-conductivity peak, presence of Poiseuille flow, and large mean free paths. On the other hand we were also able to study the effects of growth rates on our samples by variously quenching

them; that is, rapidly cooling them from melting to very low temperatures using a ^{4}He pot and dilution refrigerator. Several samples were also annealed by holding them within 10 mK of melting for several hours.

III. RESULTS AND ANALYSIS

A. Debye behavior

The thermal-conductivity data from a carefully grown 24.0 cm^3/mole sample is shown in Fig. 3. As can be seen, the data falls on a T^3 line. However this line is more significant than merely a fit to the data. The solid line is a thermal conductivity generated using Eq. (1) and is similar to the comparisons made in Fig. 1, except that in this case no adjustable parameters were used. In generating the solid line we used the specific-heat data of Greywall, the Debye phonon velocity, and a mean free path *equal* to the sample chamber diameter. The agreement is excellent over the entire low-temperature range.

In Fig. 3 we have made the comparison with the Castles and Adams data (dashed line), and have also included a comparison with recent specific-heat data of Hebral *et al.* (dotted line).[11] This latter data is at 23.8 cm^3/mole and the anomalous part of C_v seems

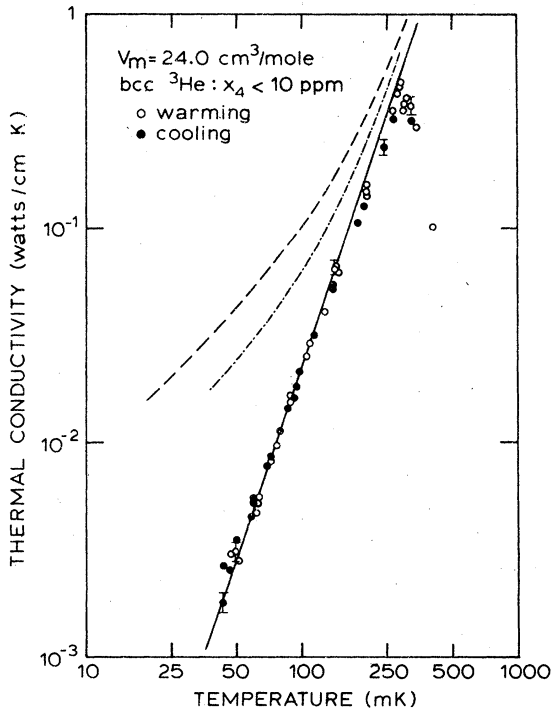

FIG. 3. Very carefully grown sample at 24.0 cm^3/mole shows a T^3 conductivity. The comparison to specific-heat data is Greywall (solid), Castles and Adams (dashed) and Hebral *et al.* (dotted).

temperature independent. For all the samples which we have grown, both T^3 and non T^3, we find the best agreement with the C_v of Greywall.

Other samples for which a T^3 conductivity was measured can be seen in Figs. 4 – 6. These samples cover the range of molar volumes 23.6 – 24.4 cm^3/mole. The latter sample, being very close to melting pressures, is therefore the sample for which anharmonic effects should be the greatest. However, as can be seen, before we manipulated the growth of this sample as we later describe, it was very much T^3.

B. Growth and annealing effects

The sample shown in Fig. 3 is the result of a very careful anneal of another sample that was first grown without special attention to the cooling rate. This latter sample had a conductivity that varied with temperature as $T^{2.8}$, and had a 20% lower conductivity maximum. The anneal was accomplished by applying heat to the mixing chamber of the dilution refrigerator. This procedure insured a uniform temperature throughout the entire sample. The sample in Fig. 3 was kept within 10 mK of melting for six hours.

It is well known that annealing increases the quality of a crystal and allows most structural defects to be minimized. Samples for which the conductivity is T^3 would then have to be considered as being closest to the defect-free crystal.

We also explored the opposite extreme of crystal preparation by quenching a sample. We cooled the sample shown in Fig. 4 as quickly as possible along the melting curve until it became all solid. This took about 20 minutes. We then continued to quickly cool the sample; the sample was below 100 mK 30 minutes after leaving the melting curve, and we allowed it to cool overnight to the lowest possible temperatures, $\lesssim 25$ mK. We made thermal-conductivity measurements as we warmed the sample the following day. The open circles in Fig. 4 show these results, and we observed a mean free path that increased with increasing temperature. We warmed to 300 mK before cooling again. This time the mean free path reached a constant value at low temperatures as expected from a boundary scattering process. Another warming cycle, the open triangles, essentially reproduced the constant low-temperature mean free path, $\lambda \approx 2$ mm. What is remarkable about this sample is that the defects that were implanted into the crystal by the quenching process were relieved during a warming from approximately 25 to 100 mK. These latter temperatures are well away from melting temperatures, ≈ 800 mK for $v_m = 24.2$ cm^3/mole. Close to melting, thermally activated diffusion is largest, and it is typically by the diffusion process that strains and structural defects are relieved. Since thermally activated diffusion decreases approximately as

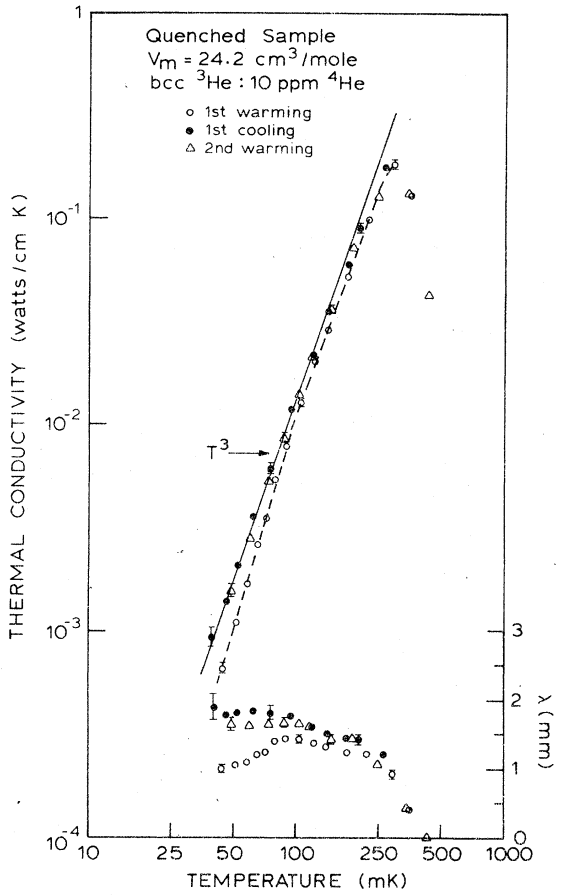

FIG. 4. Effects of rapid cooling on the thermal conductivity. Most of the additional scattering defects were relieved between 25 and 100 mK.

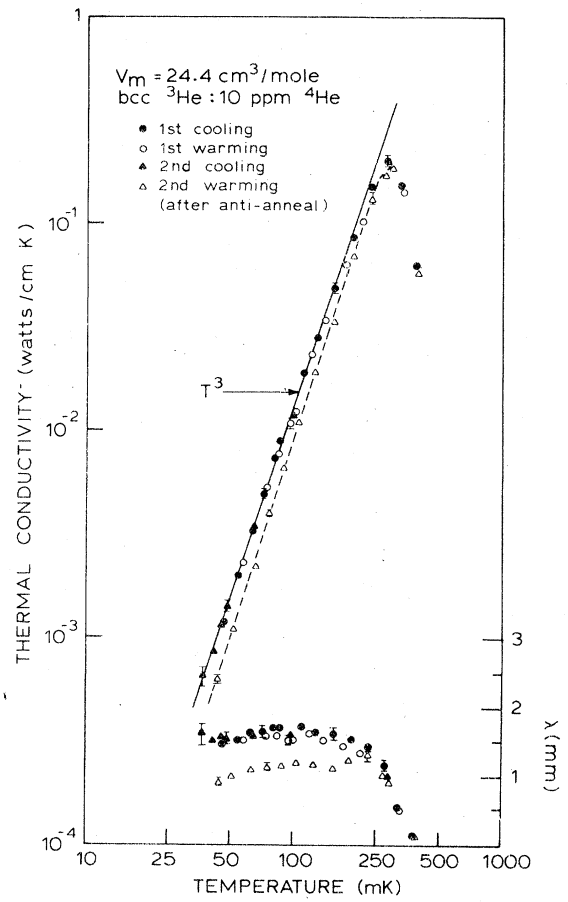

FIG. 5. Effects of melting a sample by intercepting the equilibrium melting curve at low temperature.

exp $(-W/kT)$ with $W/k \approx 10$ K in bcc ^{3}He, it is difficult to explain how this process makes a major contribution to healing for $T \lesssim 100$ mK. On the other hand, quantum tunneling in bcc ^{3}He is quite large for this molar volume with an exchange frequency $J \approx 10$ MHz. It is possible that quantum diffusion of the helium atoms through a free-energy temperature-dependent barrier associated with the strains or defects allowed the sample to heal even at very low temperatures. Within the limits of our measurements, all the other samples we formed at high temperatures did not display any metastability similar to this particular sample.

Another variation on the crystal growth procedure that we were able to perform takes advantage of one of the unique properties of ^{3}He, namely, the minimum in the melting curve. In Fig. 5 we show as the open and closed circles a sample that was formed at molar volume $v_m = 24.4$ cm^3/mole which is very close to melting density. This sample was formed by slowly cooling it from a liquid to the solid phase over a period of 12 hours. The conductivity is $k \sim T^3$, and this sample shows no signs of the defects we have observed in some of the other samples. In performing this first series of measurements we kept the lowest temperature in the sample greater than 30 mK. After three data taking sweeps that resulted in a reproducible low-temperature mean free path of 1.7 mm, we allowed the sample to cool below 25 mK. At this molar volume the sample intercepted the melting curve at ≈ 28 mK. We allowed the sample to remain in this liquid-solid state overnight. We have dubbed this process an anti-anneal, and the thermal-conductivity measurements taken upon warming from the low-temperature mixed phase are shown as the open triangles in Fig. 5. The mean free path decreased by 60%, and the gradual healing of this sample as the temperature increased from 30 to 100 mK is similar to the behavior we observed in the previous sample at $v_m = 24.2$ cm^3/mole.

C. Limited Poiseuille flow

The results of thermal-conductivity measurements on four different samples at essentially the same molar volume, ≈ 23.7 cm^3/mole, are presented in Fig. 6. This figure contains the results using two different ^{4}He concentrations, 4 and 10 ppm, and in the two different sample chambers. For all temperatures below 200 mK the data points indicated by circles fall on the solid line which is drawn as T^3. Between 200 mK and the thermal-conductivity peak at the molar volume $v_m = 23.6$ cm^3/mole (open circles) we observed a temperature dependence $k \propto T^{3.6}$ as indicated by the dashed line. This indicates a limited Poiseuille flow of phonons is taking place, and is in fact very similar to the flow observed by Thomlinson at smaller molar volumes.

An enhancement in the conductivity is made clearer when the data is displayed in terms of a mean free path using Eq. (1). We use the Debye velocity for the phonon sound velocity and the Debye temperature Θ is taken from the specific-heat data of Greywall. The resulting expression for the mean free path is

$$\lambda = 3.9 \times 10^{-5} \frac{v_m^{2/3} \Theta^2 k}{T^3} \text{ (mm)} \quad . \tag{3}$$

We show the mean free path for the $v_m = 23.6$ cm^3/mole sample in the bottom inset in Fig. 6 and have used separate symbols to distinguish between cooling and warming cycles. It can be seen that the mean free path is 20% larger in the Poiseuille region than in the boundary region and is temperature independent below 200 mK.

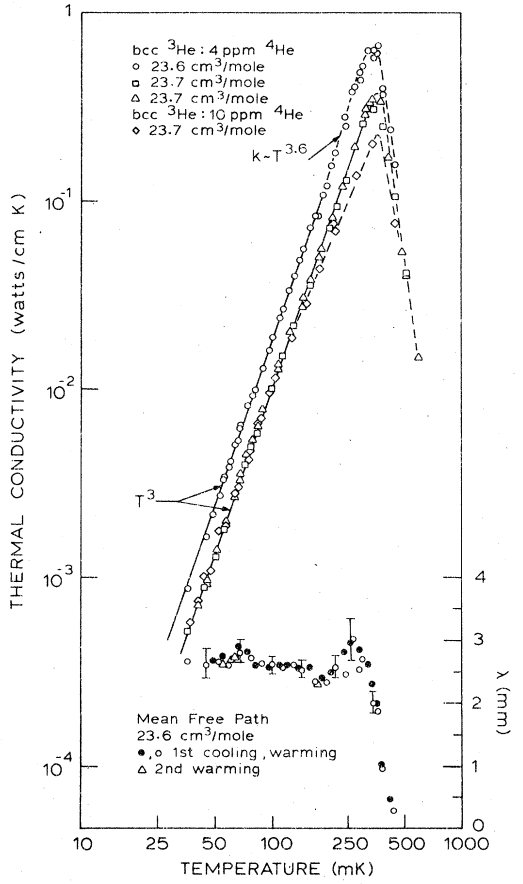

FIG. 6. Samples formed at this molar volume show $k \propto T^3$ as well as limited Poiseuille flow (upper curve) and structural defects (lower curve). The data points for the mean free path are only for the 23.6 cm^3/mole sample, but show warming and cooling cycles.

It has been generally believed that samples grown under constant volume would not be of sufficient quality to obtain sufficiently long resistive-process mean free paths such that $\lambda_R >> D^2/\lambda_N$, where D is the sample chamber or crystal diameter and λ_N is the phonon mean free path for normal processes. For the observation of Poiseuille flow it is also necessary that $\lambda_N << D$.[12] As an interesting experimental note, we believe this is the first observation of Poiseuille flow in crystals grown using the blocked capillary technique.

In defining the mean free path we have chosen to use the Debye velocity in Eq. (3). This choice is not identical to the definition of $\bar{v}$ by Casimir,[13] but it does allow us to consistently define λ for all our samples. In general, in an isotropic solid with cubic symmetry, the thermal conductivity is also isotropic.[12] However, it is possible that cubic crystals with anisotropic elastic constants will also display an anisotropic thermal conductivity.[14]

In our samples where the mean free path changed after the crystal was annealed, we have interpreted this increase in λ as due to an increase in the average crystallite dimension rather than an anisotropic effect. This is because the annealing process allows crystalline defects, such as low-angle grain boundaries, to be diminished by thermal diffusion. Since the sample is not melted during the anneal, upon recooling there will be larger sized crystallites, but the original orientation is preserved. Furthermore, thermal-conductivity measurements in the boundary scattering region of anisotropic hcp ^{4}He were found to be essentially independent of the direction of the heat flux and the crystal axis.[15]

The samples displayed as the squares and erect triangles were grown somewhat faster than the previous sample. Both samples display $k \propto T^3$ for temperatures below the conductivity maximum. We view the decreased magnitude of the thermal conductivity as due to the helium forming crystals that are on the average 50% smaller than in the previous sample. In these two samples boundary scattering is sufficiently strong to limit the resistive mean free path and Poiseuille flow is not observed.

D. Additional scattering mechanism

Also shown in Fig. 6, as the diamonds, is a sample that shows a depression in the conductivity in the temperature range 100 to 300 mK. We have plotted this depression in the conductivity as a function of temperature as the open erect triangles in Fig. 7. We computed the conductivity difference by subtracting the measured values k_m from a T^3 conductivity k_3: $\Delta k = k_3 - k_m$. The quantity k_3 is computed from Eq. (1) using the experimentally observed limiting value of the mean free path below 100 mK. The Δk's tend to fall on a single line which strongly suggests that one other scattering mechanism is present in this crystal for temperatures below the conductivity maximum.

The relatively small depression of the conductivity in the 23.7 cm^3/mole sample gives rise to the scatter in Δk in Fig. 7. For this reason we turned our attention to one of the samples that was not cubic over the entire temperature range. We chose to display the Δk results for the sample at 22.4 cm^3/mole first presented in Fig. 1. We used a mean free path *equal* to the sample chamber diameter, $\lambda = 3.07$ mm, to evaluate k_3. The results are shown as the open and closed squares in Fig. 7.

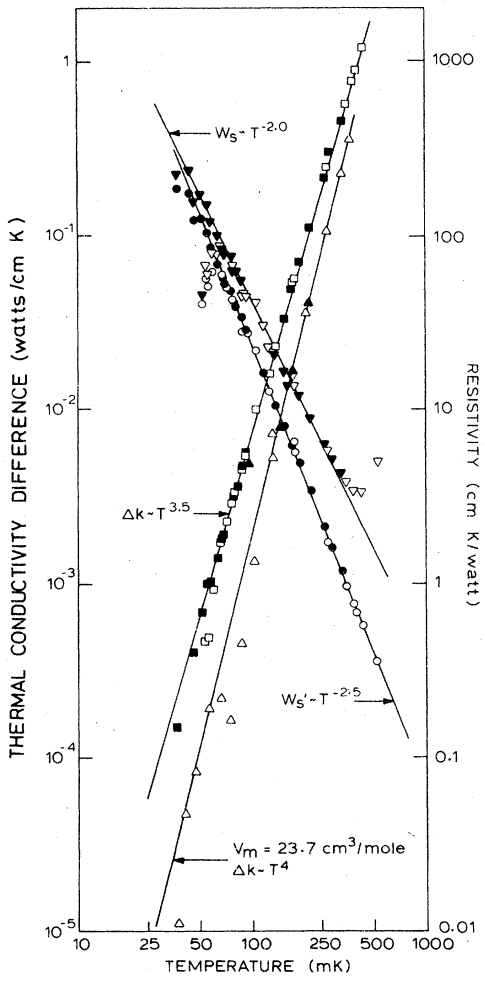

FIG. 7. Analysis of thermal-conductivity data at 22.4 cm^3/mole in terms of resistivity and depression conductivity, Δk. For $v_m = 23.7$ cm^3/mole Δk has been displaced by dividing by 10.

Once again the values for the conductivity depression fall on a straight line with a temperature dependence $\Delta k \sim T^{3.5}$. In fact, the apparent scatter in Δk below 70 mK is associated with a thermal hysteresis due to supercooling through the isotopic phase separation transition. We will give a more detailed account of thermal-conductivity measurements taken for a range of concentrations of isotopically impure helium, 4 to 500 ppm, at a later time.

In order to extract some information about the identity of the scattering mechanism it is useful to analyze the 22.4 cm^3/mole data in terms of resistivities. Using the previous definition of k_3 we can express the measured resistivity $W_m = 1/k_m$ in terms of the Debye boundary resistance W_3, and an additional resistive scattering mechanism W_s: $W_m = W_3 + W_s$. Generally, it is not correct to add resistivities because of the different phonon wavelength dependencies of different scattering mechanisms. This is especially true when phonon scattering at a boundary is one of the principal mechanisms; since, we are then adding a resistive process that is taking place at the boundary and is extrinsic to the crystal to another resistive process in which the phonons are scattered internally. With this caution in mind, we have plotted W_s as the open and closed triangles in Fig. 7. The data points tend towards a power dependence on temperature as $W_s \sim T^{-2.0}$.

Among the many authors who are aware of the pitfalls of adding resistivities, Carruthers[16] has pointed out an alternative method for extracting the resistivity of an additional scattering mechanism, which we will call W_s' to distinguish it from the previous analysis. This method is approximately valid when the depression of the conductivity due to W_s' is not large, i.e., $\Delta k/k_3 \ll 1$. Following Carruthers, we define W_s' by

$$W_m = W_3 + W_s' = \frac{1}{k_3 - \Delta k} \simeq \frac{1}{k_3} + \frac{\Delta k}{k_3^2}$$

and the additional resistivity is then $W_s' = (k_3 - k_m)/k_3^2$. We have plotted values of W_s' in Fig. 7 as the open and closed circles for the sample at 22.4 cm^3/mole. We have included points for which $\Delta k/k_3 \approx 1$ which occurs for $T \gtrsim 200$ mK, although only the lower temperature points were used in determining the slope. We find $W_s' \sim T^{-2.5}$; the same analysis on the 23.7 cm^3/mole sample gives $W_s' \sim T^{-2.0}$, while $W_s \sim T^{-1.5}$.

In other samples in which the thermal conductivity was not $k \propto T^3$ we performed the resistivity analysis

TABLE I. Summary of the power dependencies of the temperature for the analysis described in the text. The last column is the mean free path used in the analysis.

v_m(cm^3/mole)	$\frac{d\ln\Delta k}{d\ln T}$	$\frac{d\ln W_s}{d\ln T}$	$\frac{d\ln W_s'}{d\ln T}$	λ (mm)
22.4	4.2	−2.0	−2.5	3.07
22.5	3.5	−1.9	−2.3	1.30
23.7	4.5	−1.5	−2.0	1.85
24.0	3.9	−2.0	−2.2	2.80
24.3	3.8	−2.0	−2.4	2.50

for W_s and W_s' and the results are summarized in Table I. The sample at molar volume 24.0 cm^3/mole in this table is the unannealed version of the T^3 sample we have previously discussed and displayed in Fig. 3.

From Table I, we see that power dependencies of the temperature for the resistivity W_s is essentially -2. The choice of the mean free path used in this analysis does effect the temperature dependence. For example in the 22.4 cm^3/mole sample, varying λ from 2.7 to 3.1 mm resulted in the power of W_s going from 1.6 to 2.0 with similar results for W_s'. The final choice of λ presented in Table I was made consistent with limiting low-temperature values and also consistent with a resistivity that could be identified as a reasonable scattering mechanism even at very low temperatures. For any given choice of λ, the determination of the temperature exponent is not better than ± 0.1.

So far we have presented experimental evidence which indicates that when the conductivity of bcc ^{3}He is not T^3, the depression of the conductivity can be associated with an additional resistivity. This additional resistivity must be a structural defect, since it depends on the sample growth history and the effects of the defect can be annealed out of or quenched into the sample. Such evidence along with the power dependency of the resistivity suggests dislocations as the source of the phonon-scattering mechanism. We will return to this discussion after considering an analysis of the noncubic data in terms of phonon-scattering rates.

E. Relaxation rate model

In 1959, Callaway[17] introduced a phenomenological model for calculating the thermal conductivity of an insulating material. The model assumes that phonon scattering processes can be represented by a frequency-dependent relaxation rate. In 1966, Guyer and Krumhansl[12] using the linearized phonon Boltzmann equation as a starting point, arrived at an equivalent formulation of the Callaway model. In what follows we will use the equations presented by Guyer and Krumhansl because of their computational advantages.

Using the notation of Ref. 12, we can write the augmented boundary scattering rate, $(\tau_R^B)^{-1}$ due to the presence of an additional resistive process rate τ_R^{-1}, as

$$(\tau_R^B)^{-1} = \tau_R^{-1} + \tau_B^{-1} \quad . \tag{4}$$

In Eq. (4) $(\tau_B)^{-1}$ is the relaxation rate due to diffuse phonon scattering at the boundary, and we take this rate to be the ratio of the phonon velocity to the mean free path; $\tau_B^{-1} = v/\lambda$.

If we know τ_R^B we can arrive at an expression of the conductivity using Eq. (5) – (7)

$$k = \tfrac{1}{3} C_v v^2 [\langle 1|\tau_R^B|1\rangle (1-\Sigma) + \tau_z G(\mu)\Sigma] \quad , \tag{5}$$

where

$$\Sigma = 1/(1+S) \quad , \tag{6}$$

$$S = \frac{\langle 1|\tau_N|1\rangle}{\langle 1|\tau_R^B|1\rangle} \tag{7}$$

and the other terms are defined in Ref. 12.

The brackets represent an integral over phonon frequencies. For example,

$$\langle 1|\tau_R^B|1\rangle = \int_0^{\Theta/T} \tau_R^B \frac{x^4 e^x}{(e^x-1)^2}\, dx \quad , \tag{8}$$

where $x = \hbar\omega/kT$, and τ_R^B will in general be a function of x. The quantity Σ is a switching factor, and we find for the temperatures of our experiments, $T \lesssim \frac{1}{100}\Theta$, $\Sigma = 0$, and as expected, only the first term in Eq. (5) is dominant at low temperatures.

The relaxation rate model has an air of respectability surrounding it, perhaps because of its formal mathematical development. However, the usefulness of the model depends on how well a scattering mechanism can be represented by a single scattering rate. The results of our resistivity analysis indicate an additional scattering is taking place from disloca-

tions. According to Carruthers, who was only approximately able to model the microscopic scattering from dislocations, this rate is $\tau_R^{-1} \propto \omega$ for phonons scattering from the strain field of a dislocation-type defect.

In Fig. 8 we show as the dashed lines a fit to noncubic thermal-conductivity data at 22.5 cm^3/mole using the relaxation rate model. We used the expression $\tau_R^{-1} = A\omega = A(kT/\hbar)x$, and we numerically evaluated the integrals allowing A to vary to obtain the best fit. As can be seen in this figure, with $A = 3 \times 10^{-6}$ we obtain an excellent fit to the temperature dependence of the data. The magnitude of the conductivity calculated using Eq. (5) was scaled at 100 mK to agree with our experimental values. Using the same scale factor, we show in Fig. 8 the effect of a choice of A different by an order of magnitude both larger and smaller. The conductivities of the other noncubic samples were also fit using the relaxation rate model with A ranging from 2 to 3×10^{-6}.

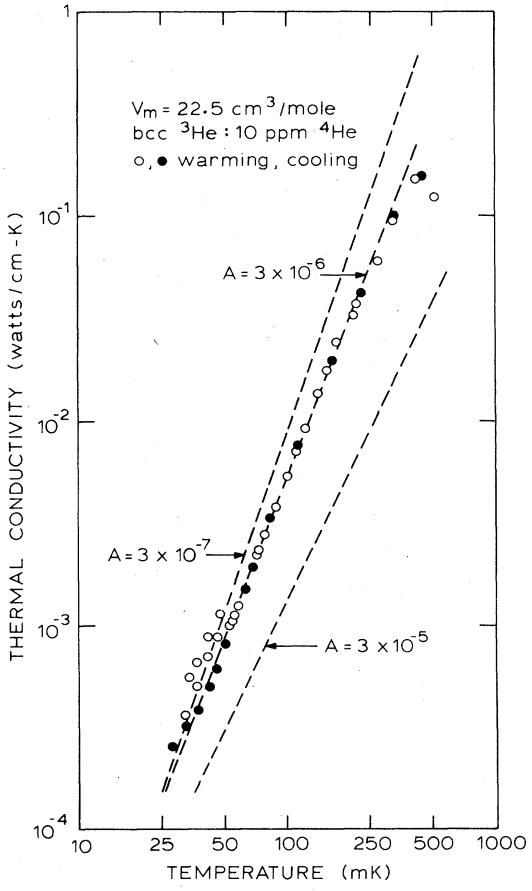

FIG. 8. Fit to non-T^3 conductivity data at 22.5 cm^3/mole using the relaxation rate model. The effect of varying the parameter A is shown.

IV. DISCUSSION AND COMMENTS

When we first began these experiments the major question in our minds was what is responsible for the noncubic behavior of the thermal conductivity in bcc ^{3}He in the limit of low temperatures. There are, in fact some very good reasons why the conductivity was not expected to be $k \propto T^3$: Theoretically, the large anharmonic force constants in bcc ^{3}He lead to finite phonon life times, thus casting the basic model of heat transport by phonons in doubt. Experimentally, we have already mentioned the thermal-conductivity measurements of Thomlinson, and the several anomalous specific-heat measurements, which when taken together, indicated $k \sim T^n$ with $n < 3$ for temperatures below k_{max}. However, we have produced samples in which we have measured $k \propto T^3$ from k_{max} to the lowest temperatures obtainable in this experiment, $T \lesssim 30$ mK. This is the major contribution of this work.

Although no systematic investigation of the effects of isotopic impurity scattering was attempted in this series of experiments, we did use two isotropic concentrations, varying from 4 to 10 ppm ^{4}He, and we did not find any evidence for an additional mass fluctuation resistivity. Such a resistivity would have an expected temperature dependence $W \propto T$ around k_{max}, and was observed by Lawson[15] for the converse situation of 10 and 20 ppm ^{3}He impurities in ^{4}He.

Perhaps even a more remarkable difference in the thermal conductivity between hcp ^{4}He and bcc ^{3}He is the observation of Poiseuille flow, albeit of limited extent, in our samples that contained 4 ppm ^{4}He impurities and which were also polycrystalline. Furthermore, in some of our samples that contained 10 ppm ^{4}He there was a suggestion of Poiseuille flow. In these latter samples, as well as the samples of Thomlinson, the conductivity was less than cubic which we now interpret as the presence of a large number of structural defects. In comparison, the observation of Poiseuille flow in ^{4}He has always been on isotopically pure ($<$ 1ppm ^{3}He) and nearly defect-free single crystals. It is plausible that the isotropic impurities are localized on or near the core of the defect strain field and do not substantially change the resistive mean free path, λ_R. Therefore, it is still possible to fulfill weak window conditions for Poiseuille flow, $\lambda_R \gtrsim d^2/\lambda_N$, $\lambda_N \ll d$, where d is a dimension on the order of crystalline sizes, or the mean distance between structural defects.

The observation of structurally related defects in some samples where k was not T^3 we now believe to be due to dislocations. Most other intrinsic scattering processes have a very small scattering cross section at low temperatures where the phonon wavelengths are long; $\lambda_{ph} \sim h\upsilon/kT \approx 2000$ Å. However, edge dislocations and the associated strain field can extend over macroscopic distances in the crystal. The core of the

dislocation, of radius r_0, is probably not effective for scattering phonons since $r_0 << \lambda_{ph}$. However, Carruthers has estimated the displacement field of an edge dislocation to vary as log (r/r_0) and would effectively scatter phonons at very low temperatures. Because of the complicated nature of dislocations and the coupling of these dislocations to the large anharmonic forces in bcc ^{3}He, it is somewhat surprising how well a simple scattering rate models this problem.

The proportionality constant A used in fitting the data to the relaxation rate was consistently in the range (2 to 3) $\times 10^{-6}$. If we think of A as a probability for a phonon to be scattered from a dislocation, then we can relate it to the ratio of the area density of dislocations to the area density of ^{3}He atoms. At 24.0 cm^3/mole this gives a dislocation density of (1.5 to 2.5) $\times 10^9$ cm^{-2}. When compared to the density of edge dislocations found on LiF by etch pit counting,[18] (2 to 5) $\times 10^7$ cm^{-2}, our density appears very large.

We can also offer some qualitative comments as to the nature of the dislocations. One observation is that edge dislocations are more likely candidates than screw dislocations in the samples we have grown. This seems to be borne out by the large size of the dislocation and the fact that we were able to anneal the defect out. Typically, screw dislocations are not amenable to an annealing process.

Another observation that seems relevant is that the noncubic thermal conductivity apparently is particular to the bcc phase. Thomlinson observed $k \propto T^3$ in hcp ^{3}He, and in Paper II we report $k \propto T^3$ in hcp ^{4}He using the same apparatus as we used in the ^{3}He measurements.[19] Evidently, the more open structure of bcc ^{3}He allows an edge dislocation to form in the crystals more easily.

The fact that we did not grow $k \propto T^3$ samples for $v_m < 23$ cm^3/mole is more likely an experimental artifact, since the solidification temperature decreases with decreasing molar volume, and our refrigeration capabilities, and consequently cooling rates, thus increase with decreasing molar volumes. As we have demonstrated, the cooling rate plays a very influential role in the formation of structural defects.

It is generally accepted among crystallographers that point defects and dislocations are interdependent. Perhaps interestingly, the presence of dislocations may bear on the problem of vacancy-induced ferromagnetism in ^{3}He. It has been estimated[20] that if there existed a sufficiently large concentration of vacancies, approximately 0.01% at ultra low temperatures, $T \approx 1$ mK, a ferromagnetic phase of bcc ^{3}He may exist. Alternatively, Papoular[21] has attempted to explain the observed magnetic transition at $T_n \approx 1$ mK in bcc ^{3}He in terms of a defect melting instability. Both theories depend on a large concentration of vacancy defects. Our experiments would indicate that growing a defect laden crystal probably increases the concentration of vacancies, and that, for example, a carefully grown bcc ^{3}He crystal may exhibit strikingly different magnetic ordering effects, if these theories are correct, than the crystal with defects.

One final comment is to compare the structural defects we have observed with the phonon scattering from an amorphous material. The phonons in an amorphous material are believed to scatter from tunneling states[22] which are related to the amorphous structure. The resistivity of these materials is characteristically $W = W_0 T^{-2}$. The coefficient of the resistivity W_0 is approximately 10^3 to 10^4 cm K^3/W. If we cast our resistivity in this form, the coefficient is ≈ 0.3 cm K^3/W. It is enticing to compare this with the magnitude of the specific heats in amorphous materials,[23] (0.4 to 0.6) $\times 10^{-6}$ J/gK^2, and the anomalous magnitude of the specific heat reported by Castles and Adams in bcc ^{3}He, (2 to 3) $\times 10^{-3}$ J/gK^2. The ratios of conductivities ($k = 1/W$) and specific heats are of similar order of magnitude. Our implication is that perhaps the low density and large zero-point motion of atoms in bcc ^{3}He give rise to a structure similar to that found in glassy materials at very low temperatures, and the extra resistivity, while well accounted for by dislocation scattering, may on the other hand be due to phonon scattering from the tunneling states of an amorphous-type structure.

ACKNOWLEDGMENTS

We would like to thank Jim Sites of our laboratory for valuable assistance in several aspects of this experiment, and also Doug Osheroff of Bell Laboratories for assistance at a critical point in the experiment. One of us (A.S.G.) would also like to acknowledge several useful conversations with Bill Thomlinson of Brookhaven National Laboratories, and the hospitality of the Centre de Recherches sur les Tres Basses Temperatures in the Centre National de la Recherche Scientifique in Grenoble during the final stage of preparation of this paper. We would also like to acknowledge the financial support of the NSF under Grants No. DMR 78-09427 and No. DMR 76-21341.

*Address during 1979: Centre de Recherches sur les Très Basses Températures, C.N.R.S., B.P. 166X, 38042 Grenoble Cédex, FRANCE.
†Present Address: Texas Instruments, Stafford, Texas, U.S.A.

[1]W. C. Thomlinson, Phys. Rev. Lett. 23, 1330 (1969).
[2]E. C. Heltemes and C. A. Swenson, Phys. Rev. 128, 1512 (1962); H. H. Sample and C. A. Swenson, Phys. Rev. 158, 188 (1967); R. C. Pandorf and D. O. Edwards, Phys. Rev. 169, 222 (1968).
[3]S. H. Castles and E. D. Adams, Phys. Rev. Lett. 30, 1125 (1973), and J. Low Temp. Phys. 19, 397 (1975).
[4]D. S. Greywall, Phys. Rev. Lett. 39, 105 (1976), and Phys. Rev. B 15, 2604 (1977).
[5]G. Armstrong, A. S. Greenberg, and J. R. Sites, Rev. Sci. Instrum. 49, 345 (1978).
[6]S. B. Trickey, W. P. Kirk, and E. D. Adams, Rev. Mod. Phys. 44, 668 (1972).
[7]A. C. Anderson, J. H. Anderson, and M. P. Zaitlin, Rev. Sci. Instrum. 47, 407 (1976).
[8]R. Berman, *Thermal Conduction in Solids* (Clarendon, Oxford, 1976).
[9]E. M. Hogan, R. A. Guyer, and H. A. Fairbank, Phys. Rev. 185, 356 (1969).
[10]E. R. Grilly, J. Low Temp. Phys. 4, 615 (1971).
[11]B. Hebral, G. Frossati, H. Godfrin, G. Schumacher, and D. Thoulouze, J. Phys. Lett. 40, L-41 (1979). More recent measurements indicate a smaller anomalous specific heat than originally were reported (private communication from B. Hebral). In which case, the heat capacity data from Hebral *et al.* would now generate a thermal conductivity closer to the solid line in Fig. 3.
[12]R. A. Guyer and J. A. Krumhansl, Phys. Rev. 148, 766 (1966); Phys. Rev. 148, 778 (1966).
[13]H. B. G. Casimir, Physica (Utrecht) 5, 495 (1938). If we assume all the phonons are diffusively scattered from the boundary, then the mean free path which we report should be reduced by approximately 5% in order to account for the finite length of the samples. If specular reflection was present we would expect a mean free path that increased with decreasing temperatures which is contrary to what we observed in the samples where $k \propto T^3$. In the samples where k is not cubic, we interpret this result as a depression in the conductivity as we explain in the text.
[14]A. K. McCurdy, H. J. Maris, and C. Elbaum, Phys. Rev. B 2, 4077 (1970).
[15]D. T. Lawson, Ph.D. thesis (Duke University, 1971) (unpublished).
[16]P. Carruthers, Rev. Mod. Phys. 33, 92 (1961).
[17]J. Callaway, Phys. Rev. 113, 1046 (1959).
[18]R. Sproull, M. Moss, and H. Weinstock, J. Appl. Phys. 30, 334 (1959). An expression for the dislocation scattering rate by P. G. Klemens, Proc. R. Soc. Lond. Sect. A 208, 108 (1951), is $\tau^{-1} = (k/\hbar) b^2 \gamma^2 N_d T x$ where b is the Burgers vector and γ is the Grüneisen constant. This expression would result in a dislocation density, N_d, smaller than we estimated by the factors $b^2\gamma^2 < 10$. However, because of the complicated nature of dislocation scattering, the expression used for the scattering rate can in any case only be considered approximate.
[19]G. Armstrong, A. A. Helmy, and A. S. Greenberg, Phys. Rev. B 20, 1060 (1979) (following paper).
[20]J. Sokoloff and A. Widom, Phys. Rev. Lett. 35, 673 (1975); R. A. Guyer, J. Low Temp. Phys. 30, 1 (1978).
[21]M. Papoular, J. Phys. (Paris) 39, C6-133, (1978); J. Low Temp. Phys. 31, 595 (1978).
[22]P. W. Anderson, B. I. Halperin, and C. M. Varma, Philos. Mag. 25, 1 (1972); W. A. Phillips, J. Low Temp. Phys. 7, 351 (1972).
[23]R. B. Stephens, Phys. Rev. B 13, 852 (1976).